(Preprint) AAS 24-128

MISSION PLANNING AND TRAJECTORY DESIGN OF ROUNDTRIP MARS TRANSFERS

Min Qu* and Patrick Chai†

NASA's Exploration Systems Development Mission Directorate has been evaluating architecture concepts that can deliver crew and cargo to Mars vicinity and return the crew safely back to Earth. A series of trade studies and sensitivity analyses are performed to explore the trade space in an effort to inform the decision of the transportation architecture for future human missions to Mars. This paper documents the tools and methods used to perform mission scans for systems that use high-thrust propulsion and provides discussion on some interesting challenges for the roundtrip transportation architecture. Results for the reference trajectories from the current analysis cycle are presented.

INTRODUCTION

The National Aeronautics and Space Administration's (NASA's) Exploration Systems Development Mission Directorate (ESDMD) has been evaluating architecture concepts for human missions to Mars, and one of the key components is the in-space transportation system that delivers crew and cargo to Mars vicinity and returns the crew safely back to Earth. The Mars Architecture Team (MAT) within ESDMD's Strategy and Architecture Office has been conducting a large number of trade studies on different in-space transportation architecture options of two major categories: hybrid high/low thrust and high-thrust transportation systems. The hybrid systems include a SEP/Chem (solar electric propulsion and chemical propulsion) system and a NEP/Chem (nuclear electric propulsion and chemical propulsion) system, and high-thrust systems include a NTP (Nuclear Thermal Propulsion) system and an all-chemical system. This paper documents the tools and methods used to perform mission scans for systems that use high-thrust propulsion, whereas the trajectory design of the hybrid system has been documented in a separate paper[1].

Two aspects of the problem must be addressed when designing roundtrip missions to Mars. First, trajectories need to be solved heliocentrically to identify launch and departure opportunities given constraints on mission duration and Mars stay time. For systems using high-thrust propulsion, mission opportunities can be identified by solving Lambert problems while stepping through a large set of time intervals. Second, maneuvers at Mars vicinity and the selection of a Mars parking orbit must also be addressed concurringly. Since the orbit tangentially captured upon arrival is typically not ideally oriented for the Earth return maneuver at departure, additional reorientation maneuvers are required to complete the roundtrip mission. MAT uses a seven-maneuver sequence called "bi-elliptic apotwist" to not only achieve orbit reorientation but also optimize the Mars

* Staff Scientist, Analytical Mechanics Associates, Inc., 21 Enterprise Parkway, Suite 300, Hampton, Virginia 23666-6413, U.S.A.
† Aerospace Engineer, NASA Langley Research Center, Hampton, Virginia 23681, U.S.A. AIAA Member.

parking orbit in order to target specific landing sites on the Mars surface. Heliocentric trajectories and Mars vicinity maneuvers are not independent of each other since the Mars arrival and departure conditions obtained from the Lambert solutions directly impact the Mars parking orbit selection and bi-elliptic apotwist maneuvers, and departure and arrival times from an optimized heliocentric trajectory may not necessarily be optimal for the entire mission. The tool currently used by MAT combines the Lambert solver and Mars reorientation and solves both problems simultaneously such that the trajectory of the entire roundtrip mission can be optimized. An example of a bi-elliptic apotwist maneuver sequence at Mars vicinity is shown in Figure 1.

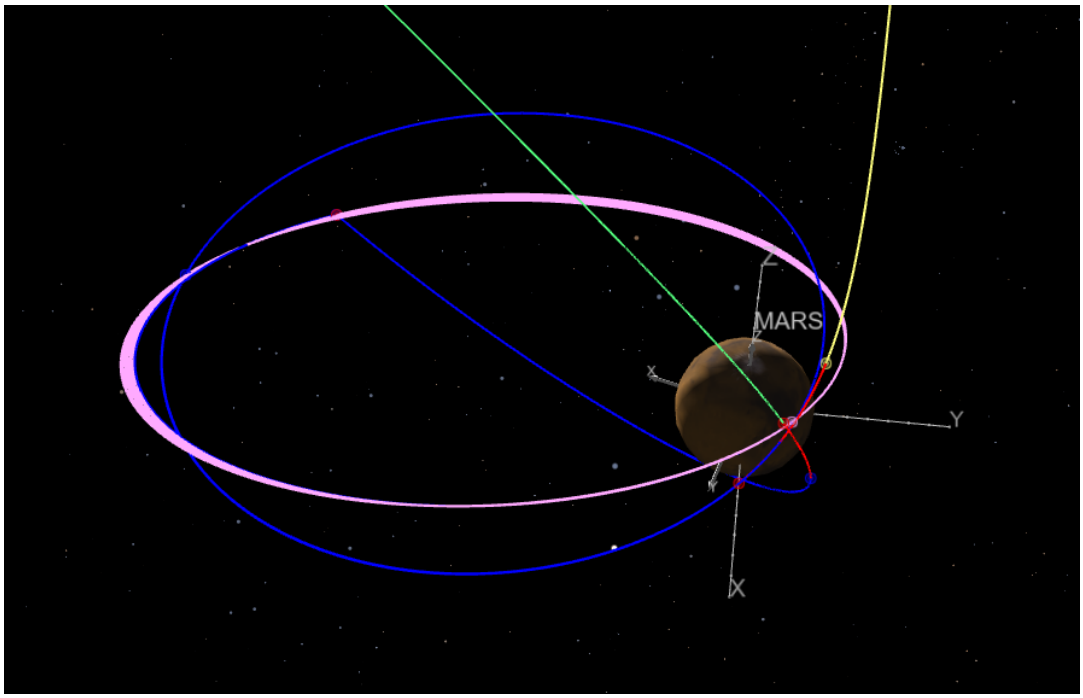

Figure 1. Example of a Mars parking orbit with bi-elliptic arrival and departure.

HELIOCENTRIC TRANSFERS

Historically, two types of Mars missions have been studied extensively. Conjunction-class missions are minimal change in velocity (ΔV) solutions and typically last three years roundtrip with a Mars stay of one year. Opposition-class missions are more costly in terms of ΔV and last less than two years with a short Mars stay. Venus flybys can sometimes be used to reduce the ΔV costs in either the outbound or inbound of the opposition-class missions. MAT is also studying other "in-between" mission options in terms of duration and stay time due to the significant duration-related flow-down impacts to crew health and performance, technology investment, development timelines, and cost[2].

Solving the interplanetary part of the trajectory is rather straightforward. For each of the outbound and inbound legs of the mission, the trajectory is assumed to contain two ballistic arcs, and they are separated by either a deep-space maneuver (DSM) or a Venus flyby. Table 1 shows a list of independent variables for the heliocentric portion of the problem solved by the optimizer. For transfers with DSMs, the input variables are departure and arrival times, time of the DSM, and the position vector of the DSM. Each ballistic arc can be solved using the Lambert solver, and the outputs are the ΔV at the DSM and the departure and arrival hyperbolic excess velocities (V_∞) at Earth and Mars. For transfers with a Venus flyby, the input variables are departure and arrival times and time of the flyby. Similar to the DSM case, the ballistic arcs for the flyby case are

solved by the Lambert solver, but the outputs are departure and arrival hyperbolic excess velocities at Earth, Mars, as well as Venus. Additional constraints on Venus flyby V_∞ magnitudes and turn angle must also be imposed to satisfy the minimum flyby distance requirement.

Table 1. Independent variables for heliocentric portion of the optimization.

Variable	Description
T_ed	Earth departure time
T_ma	Mars arrival time
T_md	Mars departure time
T_ea	Earth arrival time
T_dso	Time for outbound deep space maneuver or Venus flyby
T_dsi	Time for inbound deep space maneuver or Venus flyby
RX_dso	X component of position vector for outbound deep-space maneuver
RY_dso	Y component of position vector for outbound deep-space maneuver
RZ_dso	Z component of position vector for outbound deep-space maneuver
RX_dsi	X component of position vector for inbound deep-space maneuver
RY_dsi	Y component of position vector for inbound deep-space maneuver
RZ_dsi	Z component of position vector for inbound deep-space maneuver

Two key output variables from the heliocentric solution are total mission duration and Mars stay time because they have significant impact on the overall trajectory optimization. An extensive trade study has been performed by MAT to look at how different architecture options perform when constraints on duration and stay time are imposed. Depending on the mission and system design choices, some additional output variables may need to be constrained. For example, due to thermal limitation of the spacecraft, it may be necessary to limit the minimum distance to the Sun for the trajectory, and this can be achieved by setting a lower bound on the radius of perihelion for the ballistic arcs. The Earth departure maneuver is assumed to be from a low or elliptic Earth orbit and the ΔV can be calculated based on the departure V_∞ magnitude. The declination of the Earth departure V_∞ vector may need to be constrained such that it is less than the inclination of the initial Earth orbit, since the V_∞ vector must lie within the orbital plane of the initial Earth orbit unless an out of plane maneuver is utilized. For Earth return, it is assumed that the spacecraft will either insert itself into a final Earth orbit or perform a direct entry into Earth atmosphere. The ΔV for Earth orbit insertion is calculated based on a tangential burn at perigee from the Earth return V_∞ magnitude. The Earth return maneuver for direct entry may be eliminated if the Earth entry velocity is below the required limit, otherwise a burn is needed to reduce the V_∞ magnitude enough to satisfy the maximum entry velocity constraint.

MARS VICINITY OPTIMIZATION

The spacecraft enters Mars vicinity hyperbolically with an incoming V_∞ vector determined by the Lambert problem, performs Mars vicinity operations, and eventually leaves Mars hyperbolically with an outgoing V_∞ vector from the Lambert solution. The bi-elliptic apotwist is designed

to “connect the dots” between these critical events and facilitate transitions of orbital phases for the entire duration of the Mars vicinity stay. The methodology for optimizing the bi-elliptic apotwist has been previously discussed in 2017[3]. The set of parameters listed in Table 2 uniquely defines the Mars arrival hyperbolic orbit, intermediate bi-elliptic orbits after Mars capture, parking orbit prior to descent, parking orbit after ascent, intermediate bi-elliptic orbits prior to Mars escape, and Mars escape hyperbolic orbit. The arrival hyperbolic orbit and the first half of the bi-elliptic orbit are assumed to be co-planar and separated by the first Mars Orbit Insertion (MOI1) maneuver. The second Mars Orbit Insertion (MOI2) maneuver is the plane change, and the second half of the bi-elliptic orbit takes the spacecraft to the periapse where the third Mars Orbit Insertion (MOI3) maneuver is performed tangentially to insert the spacecraft into the Mars arrival parking orbit. The Mars departure sequence starts from the departure parking orbit and three Trans-Earth Injection (TEI1, TEI2, and TEI3) maneuvers are performed similarly to the Mars arrival sequence but in reverse order.

The outputs from the Mars vicinity stay optimization include the orbital elements of the hyperbolic, bi-elliptic, and parking orbits as well as the ΔV’s for the seven bi-elliptic apotwist maneuver sequence. The Mars arrival portion of the orbits is calculated and propagated forward (with J2) to the time of the twist maneuver (Ttwist), whereas the Mars departure portion of the orbits is calculated and propagated backwards to Ttwist, at which point the lines of apside of the arrival parking orbit and the departure parking orbit must line up so that the apotwist maneuver can be performed. The lining up of the two orbits can be achieved by constraining the angle between the two lines of apside to zero in the optimizer. Two other constraints must be imposed to ensure the geometry of the bi-elliptic maneuvers is valid. R_a and R_d, the radii of the capture and escape maneuvers MOI1 and TEI3, must be greater than the periapse altitudes of the connecting bi-elliptic orbits Rpb_a and Rpb_d such that the orbits intersect each other and the locations of the maneuvers can be solved.

Additional constraints on the parking orbits can be imposed to satisfy different mission objectives and concept of operations. For surface missions, the design of the entry, descent, and landing system may require the landing site be directly under the parking orbit periapse, which can be achieved by setting a constraint such that the declination of the arrival parking orbit periapse is equal to the landing site latitude. The longitude of the landing site can be targeted by adjusting the Mars arrival time such that the parking orbit is properly phased for landing. To minimize the mass of the Mars ascent stage, it may be desirable to set the departure parking orbit inclination to be equal to the landing site latitude such that the ascent stage only needs to perform due-east ascent to get back to the parking orbit. Another option is to have the ascent stage perform a co-planar ascent to a parking orbit with an inclination higher than the landing site latitude, which in some cases can reduce the overall ΔV cost of the transportation system, but at the cost of a slight increase in the ascent stage performance budget.

Assuming the landing site is right underneath the periapse of the Mars arrival parking orbit, the placement of the Mars arrival parking orbit is crucial to mission planning and design of the surface mission. One of the key output variables analyzed in the current MAT analysis cycle is the lighting conditions for entry, descent, and landing, which is a subject that has not been investigated in previous studies. While different landing site longitudes can be targeted with proper phasing of the spacecraft as the planet rotates underneath the parking orbit, the position vector of the landing site at the time of landing remains relatively unchanged in Mars inertial frame (MARSIAU) and so does the Sun vector. The local time of landing can be calculated based on the difference in the right ascensions between the Sun vector and the periapse position vector in the MARSIAU frame at the end of the Mars parking orbit insertion and then scaled in the 24-hour Martian clock with local time of noon being 12:00. Once the spacecraft is inserted into the park-

ing orbit, the local time of landing is determined, and it will be hard to dramatically change the local time of landing since rotating the periapse of a highly elliptic orbit can be very costly.

Table 2. Independent variables for Mars vicinity portion of the optimization.

Variable	Description
B_a	B-plane angle at Mars hyperbolic arrival
B_d	B-plane angle at Mars hyperbolic escape
Rp_a	Periapse altitude of Mars hyperbolic arrival orbit
Rp_d	Peripase altitude of Mars hyperbolic escape orbit
Ta_a	True anomaly of Mars hyperbolic arrival orbit for capture burn
Ta_d	True anomaly of Mars hyperbolic escape orbit for departure burn
Rpb_a	Periapse altitude of arrival bi-elliptic orbit
Rpb_d	Periapse altitude of departure bi-elliptic orbit
Tab_a	True anomaly of arrival bi-elliptic orbit for plane change burn
Tab_d	True anomaly of departure bi-elliptic orbit for plane change burn
Bb_a	Turn angle for arrival bi-elliptic plane change
Bb_d	Turn angle for departure bi-elliptic plane change
pp	Parking orbit period
Ttwist	Time for apotwist

REFERENCE TRAJECTORIES

MAT is conducting a large number of trade studies and is in the process of developing a set of reference trajectories that can be used to compare different Mars transportation architecture options and eventually help the stakeholders make key decisions on the future human missions to Mars. In the current analysis cycle, the initial assumption is that the elements will be launched to cis-lunar space and aggregated in an elliptical lunar-distance high-Earth orbit (LDHEO) before Earth departure. Upon Mars arrival, five-sol bi-elliptic orbits are used to insert the spacecraft into a Mars parking orbit and the period of the parking orbit is also assumed to be five sols, with a periapse altitude of 250 km. Five-sol bi-elliptic orbits are also used for Mars departure and the spacecraft will be inserted to a LDHEO upon Earth arrival. A landing site latitude of 35 degrees is used for most of the trade studies because the most likely sites for the first human mission will be in the lower latitude regions. Due-east ascent is assumed for the setup of the departure parking orbit.

Combining the heliocentric and Mars vicinity portions of the trajectories, a total of 26 independent variables and 15 constraints are set up for the nonlinear programming problem, which is solved by SNOPT[4]. The objective function to be minimized by the optimizer is the total mission ΔV, which includes maneuvers from trans-Mars injection, deep space maneuvers, bi-elliptic Mars capture and escape, and Earth orbit insertion. For each mission trajectory, the problem is solved

thousands of times with randomized initial guesses for the independent variables to ensure a globally optimized solution can be found.

Table 3 shows the optimized solutions for conjunction-class mission opportunities between 2028 and 2054. Total mission duration, Mars vicinity stay time, Earth departure declination, and local time of landing are all unconstrained in this trade study such that minimal ΔV solutions are found for all the opportunities, and they can serve as reference points for later trade runs. Total mission duration, which is the time between trans-Mars injection and Earth orbit insertion, is about 1000 days for most of the opportunities with a minimum of 945 days for the 2048 opportunity. Mars stay time, which is the time between the MOI1 and TEI3 maneuvers, has a larger variation ranging from 334 to 569 days. Deep-space maneuvers are not needed for these conjunction-class solutions since these are the least constrained problems. The total ΔV ranges from 2.95 km/s to 3.7 km/s, and about half of the solutions could potentially have difficult lighting conditions for landing because the local landing times for those trajectories have passed the average sunset time on the Mars surface of 18:00.

Table 3. Conjunction-class mission opportunities, minimizing the total roundtrip energy.

Year	Earth Departure	Mars Arrival	Mars Departure	Earth Arrival	Mars Vicinity Stay (days)	Roundtrip Duration (days)	Total ΔV (km/s)	Local time for Landing (hr)
2028	11/23/2028	09/20/2029	09/02/2030	08/19/2031	347	999	3.50	16:43
2030	12/23/2030	10/02/2031	02/17/2033	09/19/2033	505	1001	3.63	19:06
2033	04/18/2033	11/06/2033	05/10/2035	11/25/2035	551	951	3.57	20:59
2035	06/29/2035	01/20/2036	07/2/2037	03/27/2038	529	1002	3.73	20:57
2037	08/19/2037	08/03/2038	07/25/2039	05/04/2040	356	989	3.44	21:23
2039	09/19/2039	08/22/2040	08/03/2041	05/31/2042	346	985	2.95	13:43
2041	10/24/2041	09/04/2042	08/04/2043	07/02/2044	334	982	2.95	15:39
2043	11/12/2043	09/16/2044	08/20/2045	08/05/2046	339	997	3.30	16:42
2045	12/08/2045	09/24/2046	01/18/2048	08/26/2048	481	993	3.70	19:50
2048	03/26/2048	10/15/2048	03/21/2050	10/27/2050	523	945	3.69	21:27
2050	05/25/2050	12/16/2050	07/06/2052	01/10/2053	569	961	3.68	14:40
2052	08/12/2052	03/10/2053	07/20/2054	04/22/2055	497	983	3.55	17:24
2054	09/07/2054	08/15/2055	08/01/2056	05/20/2057	352	986	3.11	13:36

Table 4 shows the optimized solutions for opposition-class mission opportunities between 2030 and 2052. Opposition-class trajectories typically have a Venus gravity assist for either the outbound or inbound leg of the mission and they are marked as either EMVE (Earth-Mars-Venus-Earth) or EVME (Earth-Venus-Mars-Earth) for all the opportunities. Total mission duration, Earth departure declination, and local time of landing are also unconstrained in this trade study while the Mars stay time is constrained to be at least 50 sols. Total mission durations for opposition-class missions are typically less than two years with the 2042 EVME opportunity being the shortest at 566 days. Total ΔV is significantly higher and varies a lot more than for the conjunction-class missions, and deep-space maneuvers are required for some of the transfer legs. Four of the thirteen solutions have lighting problems for landing while the rest are favorable.

While conjunction-class missions are the most cost effective from the ΔV perspective, the long duration, long-stay nature of the trajectory may not be ideal for the first crewed mission to Mars. Opposition-class missions are short duration, short stay, but the ΔV's are much higher. Al-

so, the trajectories get much closer to the Sun and may present thermal challenges to the spacecraft design. A set of "in-between" trajectories can be found by conducting a trade study on the conjunction-class missions with constrained duration and stay times. Figure 2 shows the total ΔV as a function of total mission duration for the 2039 opportunity with a minimal Mars stay of 50 sols. Starting from the conjunction-class trajectory on the far right of the curve, the stay time is reduced to the minimal value as the duration decreases below 900 days, and the total ΔV increase more dramatically as the duration decreases further. These trajectories typically go farther away from the Sun in either the outbound or inbound leg of the transfers and require a deep-space maneuver. In the current MAT analysis cycle, a duration of 850 days was chosen as a reference to represent this class of short stay, moderate duration mission trajectories. Table 5 shows the mission opportunities for this class of 850-day duration, 50-sol stay trajectories between 2028 and 2054. Total ΔV's for this class of mission are lower than for the opposition-class and range from 4.8 to 6.7 km/s. Lighting conditions for several of the solutions may be less than ideal as they are close to the sunset time.

Table 4. Opposition-class mission opportunities, with a Venus flyby maneuver.

Year	Earth departure	Mars arrival	Mars departure	Earth arrival	DSM	Venus flyby	Roundtrip Duration	Total ΔV (km/s)	Local Time for Landing (hr)
2030EVME	01/27/2030	01/14/2031	03/06/2031	11/02/2031		07/11/2030	644	8.02	00:24
2031EMVE	12/24/2030	10/07/2031	02/06/2032	12/01/2032		07/09/2032	708	8.44	15:36
2033EMVE	04/08/2033	10/15/2033	12/05/2033	11/27/2034		06/05/2034	598	5.87	12:40
2034EVME	07/26/2034	06/30/2035	08/20/2035	05/03/2036		12/09/2034	647	7.65	13:02
2035EMVE	10/12/2034	08/16/2035	10/06/2035	08/26/2036	02/14/2035	05/06/2036	684	8.35	13:39
2036EVME	06/11/2036	05/12/2037	07/02/2037	04/01/2038		11/23/2036	659	6.58	13:15
2039EMVE	03/30/2039	01/31/2040	03/23/2040	03/19/2041	07/14/2039	10/05/2040	720	8.93	01:39
2042EVME	11/30/2042	09/25/2043	11/15/2043	06/18/2044		05/07/2043	566	7.80	03:18
2043EMVE	11/12/2043	09/14/2044	12/15/2044	09/06/2045		04/16/2045	664	8.78	15:58
2045EMVE	11/20/2045	08/21/2046	10/11/2046	08/20/2047		03/03/2047	638	6.38	15:21
2046EVME	06/13/2047	05/23/2048	07/13/2048	05/29/2049	12/29/2048	10/24/2047	716	8.79	13:12
2047EMVE	07/07/2047	06/12/2048	08/03/2048	06/25/2049	11/09/2047	01/19/2049	718	8.62	14:11
2049EVME	03/30/2049	03/25/2050	05/15/2050	11/23/2050		09/12/2049	603	5.94	12:08
2052EMVE	04/23/2052	11/27/2052	01/18/2053	01/24/2054		08/11/2053	642	7.52	01:38

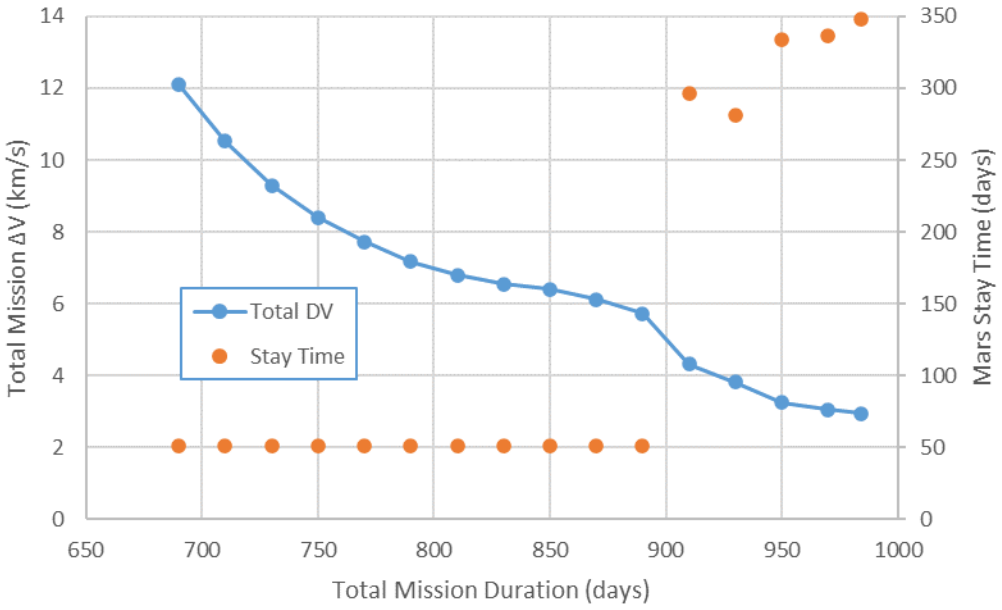

Figure 2. Total mission ΔV and stay time as a function of duration for 2039 opportunity.

Table 5. Mission opportunities for fixed 850-day roundtrip duration and 50-sol Mars vicinity stay.

Year	Earth departure	Mars arrival	Mars departure	Earth arrival	DSM1	DSM2	Total ΔV (km/s)	Local time for landing (hr)
2028	04/12/2029	09/02/2030	10/23/2030	08/10/2031	12/31/2029	03/03/2031	6.45	08:05
2031	05/17/2031	11/18/2032	01/08/2033	08/29/2033	12/11/2031		5.45	08:07
2033	07/15/2033	12/28/2034	04/05/2035	11/12/2035	03/04/2034		4.88	15:08
2035	07/04/2035	01/19/2036	03/10/2036	10/21/2037	10/12/2035	02/08/2037	4.82	16:53
2037	09/03/2037	04/12/2038	06/09/2038	12/17/2039		05/01/2039	5.87	17:44
2039	10/11/2039	07/09/2040	08/29/2040	02/07/2042	03/13/2040	04/27/2041	6.56	17:09
2041	11/16/2041	08/20/2042	10/10/2042	03/15/2044		05/05/2043	6.46	16:38
2043	12/31/2043	08/30/2044	10/21/2044	04/29/2046		06/18/2045	6.67	15:43
2045	05/11/2046	11/29/2047	01/22/2048	08/28/2048	12/27/2046		5.67	07:29
2048	06/23/2048	10/11/2049	02/28/2050	10/21/2050	01/02/2049		5.19	15:34
2050	05/26/2050	12/03/2050	01/23/2051	09/22/2052		01/05/2052	4.60	15:46
2052	08/08/2052	03/07/2053	04/27/2053	11/08/2054		03/07/2054	5.25	17:29
2054	10/03/2054	06/07/2055	07/28/2055	01/25/2057		05/08/2056	6.31	17:27

IMPROVING LIGHTING CONDITIONS FOR LANDING

Given the latitude of a landing site, the only variable that can impact the lighting condition for landing is the local time at landing, which is determined by the periapse location of the Mars

parking orbit from which the lander leaves. These MAT analyses assume that the lander performs a deorbit burn to lower the periapse altitude and targets the landing site that is directly under the periapse of the parking orbit. One potential way to alter the local landing time is to have the lander lower the periapse altitude to below Mars radius and target a landing site that is farther away from the periapse, but that would require the lander to perform a more expensive de-orbit maneuver and have a steeper flight path angle at Mars entry, which is beyond the scope of this paper. For this analysis, once the spacecraft is inserted into the elliptic parking orbit, the local time of landing is determined. For every rev the spacecraft stays in the 5-sol parking orbit, the local time for the next landing opportunity moves up 10 minutes on average due to changes in the Sun's direction relative to the parking orbit. Loitering in orbit before descending to the surface may become an option to move up the local landing time. While this average change rate of one hour per month is too slow for short-stay missions, it may be feasible for long-stay conjunction-class missions; however, loitering will cut into the crew time on the Mars surface. Another option is to adjust the placement of the Mars parking orbit by simply adding a constraint on the local landing time and letting the optimizer find a bi-elliptic apotwist solution that has more favorable lighting condition for landing.

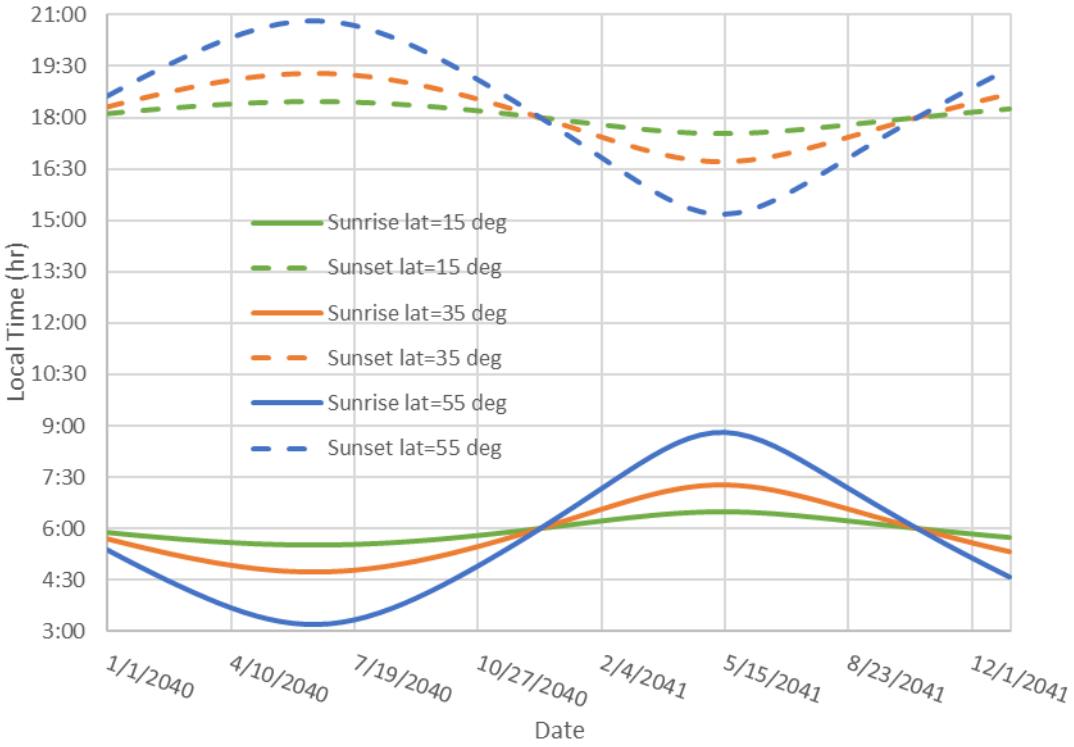

Figure 3. Sunrise and sunset times for Mars sites with 15, 35, and 55 deg latitudes.

Daylight on Mars is on average between a local sunrise time of 6:00 and a sunset time of 18:00, but it does go through seasonal changes similar to Earth as shown in Figure 3. For a landing site at 35 deg latitude, the seasonal variations can be more than an hour relative to the average sunrise and sunset times. In order to understand the performance impact of the lighting condition constraints, the trajectories for the conjunction-class missions are re-solved with additionally imposed lower and upper bounds on the local time of landing. Table 6 shows the detailed breakdown of the three solutions. Solution 0 is the original unconstrained reference solution, Solution 1

is the solution with local time of landing constrained to be between 6:00 and 18:00, and Solution 2 is the solution with local time of landing constrained between 8:00 and 16:00. Note Solution 1 may require at least a month of loiter in orbit due to the fact that the initial local time of landing is later than the sunset time of 17:01. While the inclination of the arrival parking orbit is similar for all three solutions, the ascending node of the parking orbit is shifted from 76 degrees in Solution 0 to 42 degrees in Solution 2 in order to achieve a better solar angle for the landing site. The total ΔV is increased by 0.4 km/s from 3.63 km/s in Solution 0 to 4.05 km/s in Solution 2 in order to move up the local time of landing to 15:57. The additional ΔV mainly comes from the three-burn MOI that places the spacecraft into the desired Mars parking orbit. Table 7 shows the updated conjunction-class solutions for all the opportunities between 2028 and 2054 with the local time of landing constrained between 8:00 and 16:00. Comparing to the original reference solutions, a maximum of 0.4 km/s additional ΔV is needed to ensure all opportunities have favorable lighting conditions for landing.

Table 6. Comparison of three conjunction-class solutions for 2030 opportunity.

	Solution 0 Unconstrained	Solution1 Constrained for Local Landing between 0600-1800	Solution 2 Constrained for Local Landing between 0800-1600
Earth Departure	12/23/2030	12/31/2030	12/20/2030
Mars Arrival	10/02/2031	10/14/2031	10/02/2031
Mars Departure	02/17/2033	02/18/2033	02/25/2033
Earth Arrival	09/19/2033	09/20/2033	09/22/2033
TMI (km/s)	0.580	0.539	0.593
MOI (km/s)	1.399	1.479	1.726
ApoTwist (km/s)	0.012	0.022	0.014
TEI (km/s)	0.989	1.026	1.073
EOI (km/s)	0.654	0.652	0.646
Inclination APO (deg)	38.093	39.078	35.840
RAAN APO (deg)	76.071	61.143	41.659
Total ΔV (km/s)	**3.634**	**3.718**	**4.052**
Local Time (hr)	19:06	17:51	15:57
Sunrise (hr)	6:51	6:58	6:52
Sunset (hr)	17:08	17:01	17:07

CONCLUDING REMARKS

ΔV is not the only metric to use when comparing across different transportation architectures, and spacecraft sizing and closure analyses are required to evaluate how these architecture options perform against each other. Unlike the analyses of the hybrid transportation systems where low-thrust trajectory optimizations must be performed simultaneously for different spacecraft assumptions on thrust and specific impulse, the analyses of the high-thrust trajectories are more straight forward, and the same minimal ΔV solution can be applicable to different spacecraft assumptions given otherwise the same set of mission constraints. Spacecraft sizing and closure is also simpler for the high-thrust systems because it is independent of trajectory optimization and can be performed after the minimal ΔV solution is found. However, it is not “one size fits all” because cer-

tain combinations of high ΔV cost and low specific impulse can make some mission concepts infeasible. Some architecture design options can be used to address the issue and they include using multiple stages and dropping empty tanks after major maneuvers, or pre-deploying stages at Mars parking orbits. The tools and methods described in this paper enabled NASA to evaluate both the hybrid and high-thrust architectures side by side and a series of trade studies and sensitivity analyses were performed to explore the trade space in an effort to eventually help the decision maker down select a single transportation architecture for a future human mission to Mars. Results for the reference trajectories from the current MAT analysis cycle were presented. Lighting condition for landing is an important factor and should be considered in the mission planning and design process. The bi-elliptic apotwist maneuver technique presented in this paper not only globally optimizes the roundtrip Mars mission trajectories, but also addresses constraints at Mars vicinity operations including landing site selection, lighting conditions, and ascent from the Mars surface.

Table 7. Conjunction-class solutions across mission opportunities with constrained local time at landing to enable landing in sunlight.

Year	Earth departure	Mars arrival	Mars departure	Earth arrival	Total ΔV (km/s)	Local time at Landing (hr)	Sunrise (hr)	Sunset (hr)
2028	11/22/2028	09/26/2029	09/02/2030	08/17/2031	3.58	15:44	06:19	17:40
2031	12/20/2030	10/02/2031	02/25/2033	09/22/2033	4.05	15:57	06:52	17:07
2033	04/18/2033	11/04/2033	05/18/2035	11/28/2035	3.71	13:40	07:16	16:43
2035	07/04/2035	01/23/2036	07/12/2037	04/01/2038	3.77	15:59	06:16	17:43
2037	08/15/2037	07/24/2038	07/23/2039	05/02/2040	3.56	13:30	04:43	19:16
2039	09/19/2039	08/23/2040	08/04/2041	05/31/2042	2.95	13:56	04:58	19:01
2041	10/21/2041	09/05/2042	08/09/2043	07/04/2044	2.94	15:37	05:26	18:33
2043	11/14/2043	09/18/2044	09/02/2045	08/07/2046	3.38	15:16	06:02	17:57
2045	12/07/2045	09/25/2046	01/20/2048	08/28/2048	3.98	15:36	06:36	17:23
2048	03/22/2048	10/07/2048	04/09/2050	11/06/2050	3.87	15:01	07:09	16:50
2050	05/25/2050	12/16/2050	07/06/2052	01/10/2053	3.68	14:40	06:50	17:09
2052	07/27/2052	05/03/2053	07/22/2054	04/22/2055	3.87	15:18	05:07	18:52
2054	09/06/2054	08/17/2055	08/03/2056	05/22/2057	3.11	13:28	04:50	19:09

REFERENCES

[1] M. Qu, R.G. Merrill, and P. Chai, "End to End Optimization of a Mars Hybrid Transportation Architecture," AAS Paper 9-225, 2015 AAS/AIAA Astrodynamics Specialist Conference, Portland, ME, August 2019.

[2] P. Chai, A. Sais, N. Gaug, and M. Qu, "In-Space Transportation Sensitivity to Roundtrip Mission Duration and Mars Vicinity Stay Time," AIAA ASCEND 2023.

[3] M. Qu, R. G. Merrill, P. R. Chai, and D. R. Komar, "Optimizing Parking Orbits for Roundtrip Mars Missions," AAS Paper 17-847, 2017 AAS/AIAA Astrodynamics Specialist Conference, Stevenson, WA, August 2017.

[4] P.E. Gill, W. Murray, and M.A. Saunders, "SNOPT: An SQP algorithm for large-scale constrained optimization", SIAM Review, 2005.